# List of Figures

# List of Tables

# In-cylinder charge stratification and fuel-air mixing in a new, low emission two-stroke engine

**Shamit Bakshi, Anand TNC and R.V. Ravikrishna***

Department of Mechanical Engineering

Indian Institute of Science

Bangalore 560012, India

*e-mail : ravikris@mecheng.iisc.ernet.in

**Abstract:** A new air-assisted injection system-based two-stroke engine being developed at the Indian Institute of Science, Bangalore over the past few years shows the potential to meet emission norms such as EURO-II and EURO-III and yet deliver satisfactory performance. The $70 - cc$ engine works on direct mixture injection principle with scavenging performed by air alone instead of an air fuel mixture. A small $20 - cc$ pump driven off the engine is used for mixture preparation prior to in-cylinder injection of the mixture. In the present study, the mixture injection and subsequent charge stratification process inside the engine cylinder is modeled. A three-dimensional compressible flow code with standard $k - \epsilon$ turbulence model with wall functions is developed and used for this modeling. To account for the moving boundary or piston in the engine cylinder domain, a non-stationary and deforming grid is used in this region with stationary cells in the ports and connecting ducts. A flux conservation scheme is used in the domain interface to allow the in-cylinder moving mesh to slide past the fixed port meshes. The initial conditions for flow parameters

are taken from the output of a three-dimensional scavenging simulation. The state of the inlet charge is obtained from a separate modeling of the air-assisted injection system of this engine. The simulation results show that a large, near-stoichiometric region is present at most operating conditions in the cylinder head plane. The state of the in-cylinder charge at the onset of ignition is studied leading to a good understanding of the mixing process. In addition, sensitivity of two critical parameters on the mixing and stratification is investigated. The suggested parameters substantially enhance the flammable proportion at the onset of combustion. The predicted $P - \theta$ from a combustion simulation supports this recommendation.

**Keywords** : air-assisted injection system, two-stroke engine, stratified charge engine, computational fluid dynamics

# Introduction

THE two-stroke engine is a popular choice for two- and three-wheelers owing to its simplicity, affordability and higher power-to-weight ratio. At present, there are over thirty million two/three wheelers in India alone, with an annual production of three million, which is rising every year. Over eighty percent of the two-wheelers and most of the three-wheelers in India are powered by two-stroke engines. A similar kind of statistic holds true for most of the South Asian countries. In fact, about sixty to sixty five percent of the vehicles in the South Asian region are powered by two-stroke engines. India has adopted stringent emission standards for two/three-wheelers to address the high pollution levels in Indian cities. The present emission norms allow no more than 2 gm/km of CO and 2 gm/km of HC+$NO_X$ for two wheelers in India. This is causing vehicle manufacturers to abandon the two-stroke engine owing to its high hydrocarbon (HC) and CO emissions and high brake specific fuel consumption

notwithstanding its advantages. The double firing frequency, less mechanical losses (valveless operation) and low part load pumping loss in a two-stroke engine results in a higher specific output and hence provides ready power on demand. This also results in a lower indicated mean effective pressure for a given torque in comparison to its four-stroke counterpart. Hence, the peak pressure and temperature are also lower resulting in a lower specific weight and low $NO_X$ emission. The valveless operation makes the two-stroke engine design more simple and cost effective; but direct loss of mixture during the scavenging phase and dilution of the fresh mixture with exhaust from the previous cycle results in a high brake specific fuel consumption (bsfc) and high HC and CO emissions. Direct mixture loss results in both increasing bsfc and emissions whereas dilution (particularly at part and low load conditions) results in irregular combustion and hence enhanced emissions. Thus, it is clear that a simple but effective technology for two-stroke engines is essential to revive this concept for all its advantages while meeting stringent emission norms. Over the past few years, a new two-stroke engine [1] has been developed at the Indian Institute of Science, Bangalore. The new engine shows a potential to meet future emission norms and yet deliver satisfactory performance. A detailed description of this engine has been presented before [2, 3], however, a short description of the same is included below.

The engine operates in a direct mixture injection principle and uses a simple air-assisted injection system for mixture preparation and injection. It is understood that the direct mixture loss in a conventional two-stroke engine can be largely attributed to the fact that the tasks of scavenging of combustion products and mixture injection are coupled and carried out simultaneously. Hence, separating these processes is a key consideration in addressing this problem. In other words, scavenging is performed by air alone and fuel is introduced in the appropriate phase of the cycle separately. As seen from Fig. 1, the new two-stroke engine mainly consists of (i) a Mixture

Preparation Device (MPD) and (ii) the engine. The MPD consist of the inlet duct, throttle body, inlet manifold and pneumatic pump. The inlet duct draws in air from the atmosphere which mixes with the liquid fuel in the throttle body and is carried through the inlet manifold to the pneumatic pump. The air pump piston is connected to a connecting rod and crank mechanism which is driven off the engine and at the engine speed. The pump is connected through a port with the engine cylider. Piston motion of the pump and the engine cylinder appropiately adjusts the charge injection time and duration from the pump into the engine cylinder.

A detailed modeling of the MPD [2] and the scavenging process [4] has been presented earlier. The theme of the present paper is to study the mixing and interaction of the fresh air-fuel mixture from the MPD with the in-cylinder post-scavenged air. Hence, this computation receives input in the form of state of the charge from the simulation of the MPD, and the in-cylinder flow structure from the scavenging simulation. With these initial conditions, the mixing and charge stratification process is studied using a multi-dimensional simulation.

In direct mixture injection engines, fuel-air mixture is injected after completion of the scavenging phase. Due to this delayed injection, the mixture at the onset of ignition is generally not distributed uniformly inside the engine cylinder; rather the in-cylinder charge attains a stratified state under most engine operating conditions. This has both favourable and unfavourable consequences. The advantage of operating in a stratified mode is obvious as it allows the engine to operate with an overall-lean mixture resulting in better fuel conversion efficiency and thereby improving fuel economy. However, while operating in a stratified mode, it is important to generate a near-stoichiometric mixture at the spark gap and also allow optimum mixing to ensure sufficient quantity of flammable mixture within the cylinder just prior to sparking. More importantly, this condition has to be attained over the entire operating range.

This makes the task of designing the stratified charge engine more challenging, and multi-dimensional models are required to accomplish this task. The developments of the computational tools and their application for modelling of the MPD and the scavenging process has been reported earlier [2, 4]. A detailed computational study is performed for the present engine to investigate the in-cylinder fuel-air mixing and distribution. The application of the previously developed computational methods to the charge stratification process and utilizing modeling results to develop guidelines for efficient engineering of the air-assisted injection based two-stroke engine are the subject of this paper.

# Engine Geometry and Computational Domain

The basic dimensions of the engine are given in Table 1. The typical values of fuel and air flow in the system ranges between $2 - 3$ $mm^3/cycle$ and $30 - 35$ $cc/cycle$, respectively, under full load conditions. The engine operates in a speed range of $2000 - 6000$ rpm and an overall equivalence ratio between $0.5 - 1$. The computational domain for the engine is shown in Fig. 2. It consists of the engine cylinder, two scavenging ports and one exhaust duct all of which are treated as separate computational blocks. Apart from the scavenging port and the exhaust duct, there is also a boost port. The injection port through which fresh air-fuel mixture is pumped into the engine cylinder is also shown in this figure. This port remains inactive for the duration of scavenging simulation. However, it is active during the injection phase and once again gets deactivated once the injection is over. In all, 22,500 computational cells are used in the scavenging port domain, 47,089 cells in the engine cylinder domain, 18,750 cells in the exhaust port domain, 12,000 cells in the boost port domain and 14,000 cells in the injection port domain.

| | |
|---|---|
| **No. of Cylinders** | Single |
| **Displacement Volume** | 70 $cm^3$ |
| **Bore, Stroke**<br>**Connecting rod length** | 46 $mm$, 42 $mm$<br>84 $mm$ |
| **Crankcase volume** | 130 $cm^3$ |
| **Piston crown opening and closing timing for exhaust and scavenging ports** | $114^O$ ATDC/ $246^O$ ATDC (exhaust port)<br>$135^O$ ATDC/ $225^O$ ATDC (scavenging / boost port) |
| **Port width** | 25 $mm$ (exhaust)<br>25 $mm$ (scavenging) |
| **Port angles** $(\theta_y, \theta_z)$ **(refer Fig. 2)** | $50^O$ and $25^O$ |
| **Port angles** $(\theta_b, \theta_i)$ **(refer Fig. 2)** | $45^O$ (both) |

**Table 1**: *Geometric details of the engine configurations*

# Computational Methodology

The injection and mixing processes of the gaseous fuel-rich mixture are subsequent to the scavenging process [4]. The injection port is treated as a new domain and the port interface is treated using the moving mesh and multi-block algorithm, the development of which was discussed earlier [4]. This algorithm is based on the moving mesh mesh method of Peric [5] in conjunction with the zonal boundary scheme of Rai [6].The details of the various stages of the computation from the scavenging port opening to the onset of sparking are presented in Table 2.

It is observed from Table 2 that the computation is carried out in five important stages. The abbreviations used for representing the active domains in the Table are, '$Cyl$' for the engine cylinder, '$SP$' for the scavenging port, '$EP$' for the Exhaust port, '$IP$' for injection port, and '$BP$' for the boost port. The entire computer program was written in Fortran-90 language where the use of dynamic arrays is a desirable feature for this kind of multi-block computation. For example, as seen from Table 2,

| Computation Stage | Crank Angle | Event | Active Domains |
|---|---|---|---|
| 1 | $135^O$ ATDC- $225^O$ ATDC | Scavenging | 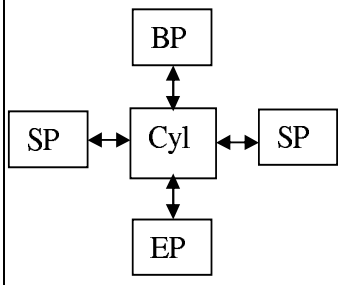  |
| 2 | $225^O$ ATDC- $235^O$ ATDC | Scavenging continues with closure of scavenging and boost port | 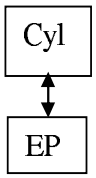  |
| 3 | $235^O$ ATDC- $246^O$ ATDC | Charge Injection starts | 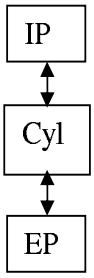  |
| 4 | $246^O$ ATDC- $270^O$ ATDC | Injection continues | 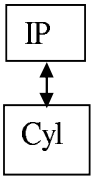  |
| 5 | $270^O$ ATDC- $340^O$ ATDC | Compression |   |

**Table 2**: *Details of the various stages of computation of the in-cylinder phenomena.*

the boost port ($BP$) and the Injection port ($IP$) are never simultaneously active and hence all variables related to these blocks can be stored in a single dynamic array which will adjust to the required size as and when required. During stage-5, the computational domain is re-discretized a couple of times owing to the necessity of maintaining the aspect ratio of the control volume between 0.5-2.0 to avoid numerical instabilities [7].

## Boundary and Operating Conditions

A typical computational domain corresponding to $15^{\mathrm{O}}$ BBDC, i.e., stage-1 of the computation (Table 2) is shown in Fig. 2. All domains except the injection port are active under this condition. The computational domain at $100^{\mathrm{O}}$ ABDC is shown in Fig. 3 and the engine cylinder is the only active domain under this condition corresponding to stage-5 of the computation sequence (Table 2).

### Boundary Conditions

One end of the injection port is connected to the pneumatic pump and the other end is connected to the engine cylinder. The piston of the pneumatic pump is close to TDC when the injection process commences. Hence, the pump volume during the injection phase is very close to its clearance volume, which is very small. Hence, to save on computational time, the pump is treated as a zero-dimensional entity during the present computation. Pressure and vapour mass fraction is specified as a boundary condition in the pump end of the injection port. The pressure-time information is obtained from the zero-dimensional analysis and used as a boundary condition for the pump end of the injection port. The vapour mass fraction at the pump end is computed from the analysis of the air-assisted injection system as presented earlier [2].

The equivalence ratio ($\phi$) specified for a typical operating condition is presented in the next section.

### Operating Conditions

As mentioned earlier, computations are carried out at different operating conditions. Load and speed are the two important operating conditions in the context of IC engines. Depending on the driving and road conditions, the engine has to respond to various combinations of load and speed. Typically, the load can vary from idling to conditions involving steep uphill climb, and the speed can vary from idling speeds to excess of 6000 rpm. The abbreviations used for the different operating conditions, and the speed, delivery ratio and equivalence ratio corresponding to these condition are given in Table 3.

| **Operating Condition** | **Abbreviation** | **Speed** | **Delivery Ratio** | **Equivalence Ratio** |
|---|---|---|---|---|
| High Speed and High Load | HSHL | 6000 | 0.7 | 2.3 |
| High Speed and Low Load | HSLL | 6000 | 0.1 | 1.0 |
| Low Speed and High Load | LSHL | 2000 | 0.7 | 2.66 |
| Low Speed and Low Load | LSLL | 2000 | 0.1 | 1.2 |
| Mid Speed and Mid Load | MSML | 4000 | 0.4 | 1.8 |
| High Speed and Mid Load | HSML | 6000 | 0.4 | 1.8 |

**Table 3**: *Description of the operating conditions.*

# Results and Discussion

The main objective of this study is to evaluate the mixing and distribution of charge inside the engine cylinder. An appropriate level of mixing is essential to ensure sufficient quantity of flammable mixture inside the cylinder at the onset of sparking; whereas, optimum charge distribution will ensure that a stoichiometric charge is reliably located in the spark gap at all operating conditions. The results pertaining to the distribution of charge will be presented as the spatial variation of equivalence ratio in the X-Z plane (refer Fig. 2) near the cylinder head at the onset of sparking. The mixing results will be presented as temporal variation of the mass fractions of rich, flammable, lean and too lean mixture inside the engine cylinder. Initially, the flow field results indicating the flow path of the injected charge will be presented. Then, results for various operating conditions will be presented and their implications on engine performance at various conditions will be discussed. The section ends with a parametric study, where the effect of various parameters will be studied and recommendations for a better design will be proposed. Validation of the computational tools developed has been reported earlier [2, 4]. Furthermore, grid independence studies were also performed and results reported in the next sections were found to be fairly grid independent.

## Study of the Flow Field and Dependence on Operating Conditions

The charge injection into the engine cylinder commences at $235^{O}$ ATDC and is completed at $270^{O}$ ATDC. The exhaust port closes at $246^{O}$ ATDC. The velocity vector and the equivalence ratio colour map in the central Y-Z plane at $243^{O}$ ATDC and HSHL condition is shown in Fig. 5. The rapidly outgoing flow through the open

exhaust is visible in this figure. Figure 6 shows the injected jet just after the exhaust port closure from which it is clear that there is no throughput loss of the injected charge at a high engine speed. This corresponds to the base engine configuration where the charge is injected at $45^{O}$ from the plane of the piston. Similar observation is made at a low speed condition for the base engine. However, a reduction in the charge injection angle can lead to throughput loss at low speeds; hence, such a configuration is undesirable for this engine. The jet expands and strikes the cylinder head at $252^{O}$ ATDC as seen from Fig. 7. At $270^{O}$ ATDC, i.e., when the injection port completely closes the jet could be seen to have completely broken down (Fig. 8) and the injected charge flows along the cylinder wall and gets reflected back from the piston head. It is seen from Fig. 9 that most of the charge moves towards the injection end top corner after getting reflected from the piston head. Figure 10 shows the charge distribution in the X-Z plane at $340^{O}$ ATDC which corresponds to the time of sparking. At this point, the charge is observed to propagate from the injection side to the exhaust side along the cylinder head. It is also observed that the charge equivalence ratio is relatively richer on the side opposite to the side towards which it was injected. The significance of this observation is that, even if the charge is directed towards the spark plug during injection, the final charge may be lean or even non-flammable at the spark gap during ignition. One important and encouraging observation from this figure is that there is a large near-stoichiometric region existing in the cylinder head plane at HSHL condition, although most of it is located on the side containing the injection port. From the study of the flow field, the flow path of the injected charge at a high engine speed is depicted in Fig. 11 (arrows in sequence from A to F show the flow path of the injected charge). At high speed, there is no interaction between the injected charge and that reflected from the piston surface, i.e., A and E in the figure. But at low speed, there is enough time and the injected jet gets deflected by the reflected

charge. This was clearly observed from the flow structure corresponding to an engine speed of 2000 rpm at $252^{O}$ ATDC (flow structure at the same crankangle at 6000 rpm is shown in Fig. 7). The charge distribution near the cylinder head prior to ignition at low speed (LSLL) is also investigated. A nearly homogeneous and near-stoichiometric (lean) charge is seen to exist in the entire cylinder head region. However, the direction of flow is seen to be opposite to that in the high speed case. This is due to the fact that the flow path at low speed condition is quite different compared to that at high speed condition which in turn is due to the interaction between the reflected and injected charge. The flow path at low speed condition is shown in Fig. 12. Thus, it is clear from the study that the injected charge finally flows along the cylinder head but approaches from the injection side at high speed and from the exhaust side at low speed. With the present injection timing, at high engine speed, the charge can sweep through more than half of the cylinder head region and at low engine speeds, the charge sweeps the entire cylinder head region. However, with delayed injection, a stoichiometric mixture can be established in exactly opposite side of the cylinder at high and low speeds. But with the present injection timing, as a near-stoichiometric mixture can be established in a considerably large region on the cylinder head over a wide range of operating conditions (from HSHL to LSLL), delaying the injection is not required for the present configuration.

Next, the dependence of mixing in the base engine on different operating conditions will be studied. Here, a rich mixture is defined for $\phi$ above 1.3, flammable mixture for $\phi$ between 0.7 and 1.3, lean mixture for $\phi$ between 0.4 and 0.7, and too lean mixture for $\phi$ below 0.4. Before discussing the results, it is useful to consider the phases in which the mixing process progresses as shown in Fig. 4 [8]. At the beginning of injection, in any direct mixture injection system, there is air, exhaust and rich mixture inside the cylinder; whereas, on complete mixing, there will be ei-

ther a homogeneous flammable or lean mixture. But, if less time is available and a stratified mixture is established, a higher thermal efficiency due to lean burning can be achieved. Higher the proportion of flammable mixture in the stratified charge, better will be the combustion stability.

As shown in Fig. 4, the rich mixture first gets converted to flammable and then to lean mixture along path-1, whereas along path-2, air and exhaust gets converted to too lean, and then to lean mixture. A reverse conversion of lean to flammable or too lean is also possible. Depending upon various factors (discussed later) like time availability, mixing intensity, etc., the final proportion of these mixtures inside the engine cylinder is determined.

Figure 13 shows the variation of mass fraction of these mixtures with crankangle for HSHL condition. Initially, the rich mixture is high in proportion which comes down rapidly and thereby enhances the proportion of the flammable and lean mixture. After a certain time, flammable mixture also gets converted to lean and its own proportion decreases increasing the proportion of lean mixture. In Figs. 14 - 15 the mass fraction variation with crank angle for LSLL, MSML conditions are presented, respectively. The low load condition is typically characterized by conversion of flammable to lean mixture at a high speed and lean to flammable mixture at a low speed. The MSML curve is quite similar to the HSHL condition, i.e., it is characterized by conversion of rich to flammable and flammable to lean mixture. The summary of the dependence on operating conditions in terms of the mass fraction of different mixtures at the onset of combustion is presented in Table 4. It is seen from Table 4 that rich mixture is generally not retained prior to ignition, except for HSHL and MSML conditions; the amount retained is quite low even for these conditions. At LSHL condition, the engine is expected to deliver high torque which appears possible from the results tabulated. However, at HSHL, MSML and HSML conditions, from the results it appears that

| **Operating Conditions ⇒** / **Mass Fraction ⇓** | **HSHL** | **HSLL** | **LSHL** | **LSLL** | **MSML** | **HSML** | **HSLL** (un-throttled) |
|---|---|---|---|---|---|---|---|
| **Rich** mixture (%) | 5.4 | 0 | 0 | 0 | 0 | 1.15 | 0 |
| **Flammable** mixture (%) | 48 | 52.7 | 100 | 84 | 52.9 | 53.57 | 1.58 |
| **Lean** mixture (%) | 34.6 | 42.92 | 0 | 16 | 44.52 | 36.37 | 34.37 |
| **Too lean** mixture (%) | 11.9 | 4.35 | 0 | 0 | 2.58 | 8.91 | 64.05 |

**Table 4**: *Summary of the results for different operating conditions - Mass fraction of the various mixtures at the onset of spark ignition.*

there might be a deficiency in torque. This observation reinforces the previously stated speed dependence of engine torque as has been presented earlier [2]. As the air and mixture inlets are separate in this engine, it is possible to operate the air line unthrottled with the added benefit of reduced pumping losses. But as observed in the last column of Table 4, an unthrottled operation at HSLL condition can excessively increase the proportion of too-lean mixture and minimize the flammable mixture prior to ignition which is undesirable. Hence, this is not a desirable option for the engine.

Next, an attempt is made to explain these trends observed at various operating conditions. There are primarily four factors which influence the mixing and hence determine the state of air-fuel mixture prior to ignition. These factors and their relative dominance at different operating conditions are shown in Table 5. It is observed from Table 5 that higher initial charge richness and lower turbulence level at low speed generally result in a higher flammable mixture at the onset of combustion

| Operating Conditions ⇒ | HSHL | HSLL | LSHL | LSLL |
|---|---|---|---|---|
| **Factors determining the state of air-fuel mixture** ⇓ | | | | |
| **Time availability** | Low | Low | High | High |
| **Initial charge equivalence ratio** | 2.3 | 1.0 | 2.66 | 1.2 |
| **Turbulence level** | Highest | Moderate | Low | Lowest |
| **Residual gas fraction** | Low | High | Low | High |

**Table 5**: *Relative dominance of factors influencing the mixing.*

in comparison to high speed. In other words, flammable mixture at low speed contains more charge with richer-than-stoichiometric equivalence ratio and hence will not easily get converted to lean mixture. Increasing the richness of the inlet mixture at high speed is also not recommended, as the rich mixture does not fully get converted due to less residence time at high speed. Higher residual gas fraction and lower turbulence level at low load results in good amount of flammable mixture present prior to ignition.

## Effect of injection angle and pressure

In this section, the effect of two crucial parameters will be studied with a view to obtain improved engine performance. From the study performed so far, it is observed that the distribution of charge at the onset of sparking is satisfactory in this engine over a wide range of operating conditions due to a large region near the cylinder head having a near-stoichiometric equivalence ratio. But, mixing and state of the charge prior to ignition need to be improved, especially at high and mid-speed conditions. Here, the study is performed for the MSML condition at which the vehicle is likely to operate most of the time. But, any improvement has to make sure that the inherent

advantages of the favourable charge distribution are retained.

At first, the angle of charge injection from the plane of the piston is varied. As indicated before, a reduction in this angle will lead to throughput losses of the charge at low engine speed; hence the effect of increasing the angle is only studied here. The variation of mass fraction of the various mixtures with injection angle is shown in Table 6. Increasing the angle of injection with respect to the plane of the piston drastically reduces the proportion of flammable mixture inside the engine cylinder and increases the proportion of lean and too-lean mixture.

| **Direction of Injection ⇒** / **Mass Fraction (prior to combustion)** ⇓ | $45^{\mathbf{o}}$ | $55^{\mathbf{o}}$ | $65^{\mathbf{o}}$ | $75^{\mathbf{o}}$ |
|---|---|---|---|---|
| **Rich Mixture (%)** | 0 | 0 | 0 | 0 |
| **Flammable Mixture (%)** | 52.9 | 4.37 | 1.29 | 0.46 |
| **Lean Mixture (%)** | 44.52 | 82.23 | 55.26 | 26.8 |
| **Too Lean Mixture (%)** | 2.58 | 13.4 | 43.45 | 72.26 |

**Table 6**: *Dependence of mixing on direction of charge injection into engine cylinder.*

This drastic reduction in the proportion of flammable mixture with increasing injector orientation can be explained by considering the structure of the injected jet with increased angle of injection. Figure 16 shows the jet structure for an injection angle of $75^{\mathrm{O}}$ at $252^{\mathrm{O}}$ ATDC. The jet is seen to adhere with the wall due to the jet-wall interaction. This happens due to the well-known Coanda effect. The jet entrains fluid from the space between the jet and the wall and hence forms a low pressure zone there. The resulting pressure difference across the jet pushes it towards the wall. This tendency of the jet to adhere to the wall substantially reduces mixing and

hence reduces the proportion of flammable mixture during ignition. Hence, injector orientation is not recommended for alteration from the existing value in the base engine.

Next, the effect of injection pressure is investigated. This can be achieved by locating the transfer port of the pump (of the MPD) closer to the TDC of the pump. Thus, delaying injection in the pump would cause the charge pressure to increase. However, the position of the port with respect to the engine cylinder should remain unchanged by ensuring an appropriate change in the phase lag between the engine cylinder and the pump. The results of this study are presented in Table 7. For the base engine, injection starts at $40^{\mathrm{O}}$ BTDC of the pump.

| **Pump crankangle (BTDC) at Injection ⇒ (BTDC of Pump)** | $25^{\mathbf{O}}$ | $30^{\mathbf{O}}$ | $35^{\mathbf{O}}$ | $40^{\mathbf{O}}$ | $52^{\mathrm{O}}$ | $55^{\mathrm{O}}$ |
|---|---|---|---|---|---|---|
| **Mass Fraction (prior to combustion) ⇓** | | | | | | |
| **Rich Mixture (%)** | 0 | 0 | 0 | 0 | 0 | 0 |
| **Flammable Mixture (%)** | 99.55 | 89.51 | 71.95 | 52.9 | 18.38 | 14.56 |
| **Lean Mixture (%)** | 0.45 | 10.47 | 27.99 | 44.52 | 69.2 | 70.7 |
| **Too Lean Mixture (%)** | 0 | 0 | 0 | 2.58 | 12.4 | 14.73 |

**Table 7**: *Dependence of mixing on injection pressure.*

Advancing the injection or reducing injection pressure is seen to substantially reduce the proportion of flammable mixture whereas delaying the injection enhances it substantially. This is because the high pressure injection delays the breakdown of the injected jet, as a consequence of which a lesser proportion of the flammable mixture becomes lean on mixing. Hence, a higher injection pressure achieved through

a delayed injection from the pump can substantially improve the flammable mixture proportion while retaining a favourable charge distribution. This is because the injection point with respect to the engine cylinder is still retained at $235^{O}$ ATDC.

# Combustion Modeling

To study the extent of improvement in engine performance with the proposed change in the injection pressure, a combustion calculation is conducted with the results of the previous computation as an initial condition. The characteristic-time model of Abraham et al. [9] is used to estimate the heat release rate and $P-\theta$ variation during the combustion process. This computation is started from $20^{O}$ BTDC and is completed at $40^{O}$ ATDC.

## Prediction of Pressure-Time Variation

Starting with the stored variables at $20^{O}$ BTDC, the computation is restarted. Ignition is achieved by specifying ignition source term for energy equation at the spark plug location continuously for ten consecutive time steps as suggested by Kuo et al. [10]. Figure 17 shows the variation in cylinder pressure with crankangle for MSML conditions. The dashed line is for the base engine with the charge injection at $40^{O}$ BTDC of the pump; whereas, the solid line is with the proposed modification of higher injection pressure corresponding to injection at $25^{O}$ BTDC of the pump. It is observed from the results that the maximum pressure for the latter configuration is much higher than that for the former case. The area under the curve from $40^{O}$ BTDC to $40^{O}$ ATDC is also found to be significantly higher for this case suggesting an enhanced torque with the proposed modification for the same operating condition (MSML). A similar observation is evident for the HSHL condition which is observed

from Fig. 18. Hence, the results of the combustion modeling support and reinforce the recommendation made before. It is also evident that apart from the speed dependence of the mixture preparation unit, another important reason for low torque at high speed in the original engine is reduced availability of flammable mixture prior to ignition.

# Conclusions

The charge injection and stratification in the air-assisted injection based engine is simulated and analyzed. The injected charge is observed to flow in different paths at different engine speeds; however, a large near-stoichiometric region is seen to be present at most operating conditions near the cylinder head region. A study of the state of charge at different operating conditions shows that at the onset of spark ignition, most of the charge is in flammable state at low speed (both high and low load), whereas about 50% of the charge is flammable at high and mid-speed conditions. A change in the injector orientation from that in the base engine results in reduction of the flammable proportion of the charge. Increasing the injection pressure by delaying injection with respect to the pump crank angle is seen to enhance the flammable proportion substantially indicating a possible improvement in the engine performance in terms of torque. A combustion modeling supplements this proposition in terms of an improved $P - \theta$ variation.

# References


[1] Narasimhan M. V., Raman N., and Venkataraman M. K., "Fuel efficient and low emission two stroke gasoline engine," *SERC, Research Highlights, Department of Science and Technology, India*, January 2000.

[2] Bakshi S. and Ravikrishna R.V., "Multidimensional simulation of the air-flow and fuel transport process in the air-assisted injection system of a new, low-emission two-stroke engine," *Proc. Instn. Mech. Engrs, Part D: J. Automobile Engineering*, vol. 217, no. 6, pp. 383–392, 2003.

[3] Bakshi S., "Modeling of thermo-fluid dynamic processes in a new, low-emission two-stroke IC engine," *Dissertation for Doctor of Philosophy, Dept. of Mechanical Engg., Indian Institute of Science, Bangalore*, September 2003.

[4] Bakshi S., Deshmukh D., and Ravikrishna R.V., "Multidimensional modelling of flow through piston-controlled ports using a multi-block, moving mesh algorithm," *Proc. Instn. Mech. Engrs, Part C: J. Mechanical Engineering Science*, vol. 218, pp. 207–222, 2004.

[5] Demirdzic I. and Peric M., "Finite volume method for prediction of fluid flow in arbitrarily shaped domains with moving boundaries," *International Journal for Numerical Methods in Fluids*, vol. 10, pp. 771–790, 1990.

[6] Rai M. M., "A conservative treatment of zonal boundaries for Euler equation calculations," *Journal of Computational Physics*, vol. 62, pp. 472–503, 1986.

[7] Ferziger J. H. and Peric M., "Computational methods for fluid dynamics," *Springer, Berlin, Germany*, 1997.

[8] Abraham J., Magi V., Maclnnes J., and Bracco F. V., "Gas verses spray injection: which mixes faster?," *SAE Paper 940895*, 1994.

[9] Abraham J., Bracco F. V., and Reitz R. D., "Comparisons of computed and measured premixed charge engine combustion," *Combustion and Flame*, vol. 60, pp. 309–322, 1985.

[10] Kuo T. W. and Reitz R. D., "Computation of premixed-charge combustion in pancake and pentroof engines," *SAE Paper 890670*, 1989.

# FIGURES

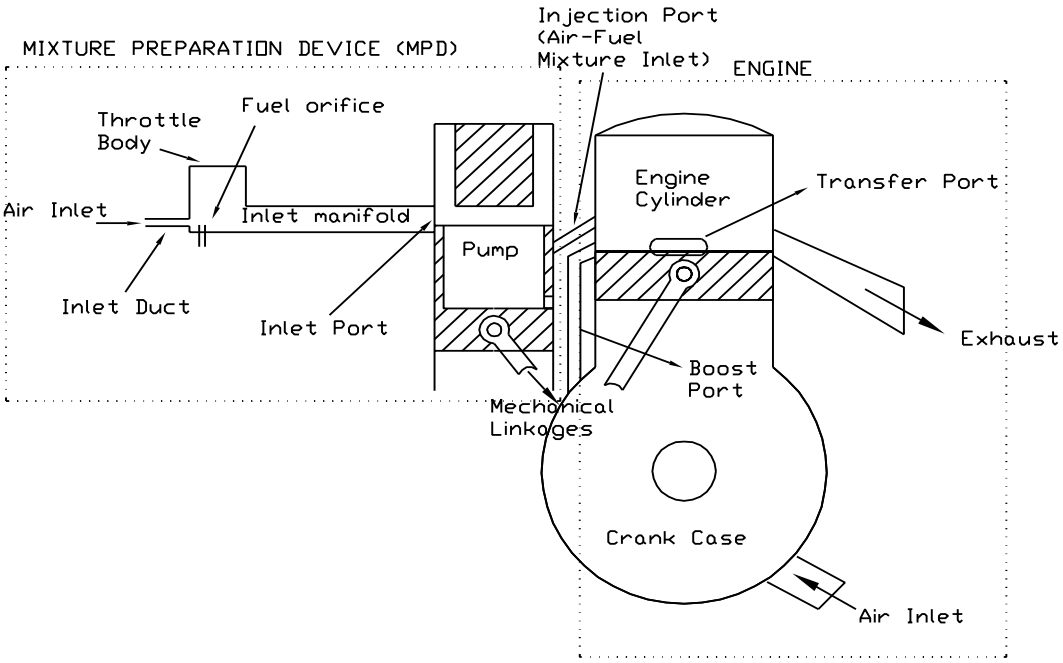


**Figure 1**: *Schematic of the air-assisted crankcase scavenged two-stroke engine.*

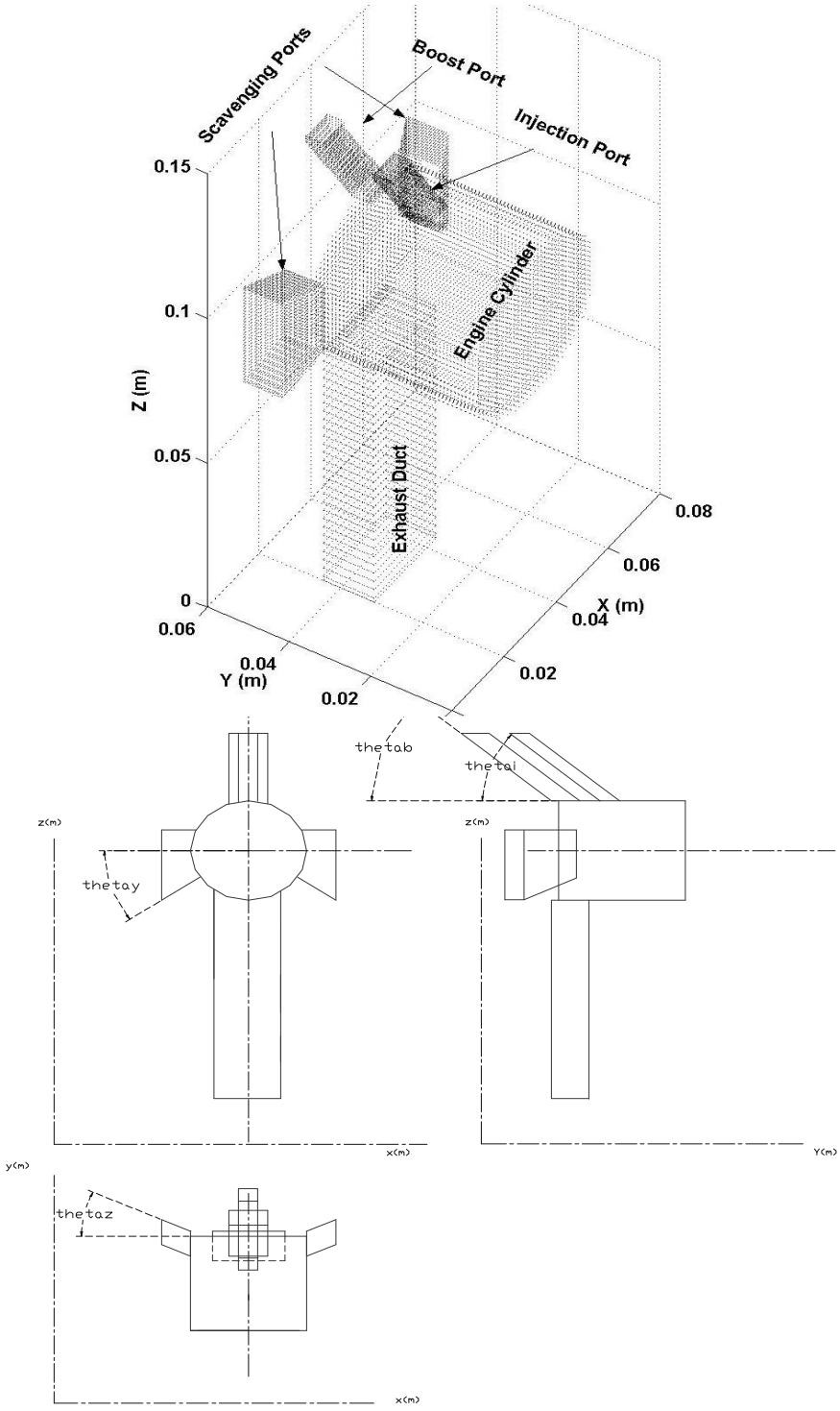


**Figure 2**: *Geometry of Engine-2 (70-cc) for which scavenging modeling is performed. Three-dimensional geometry is shown in the top-half of the figure and projections in x-z, x-y and x-y plane are shown in the bottom-half.*

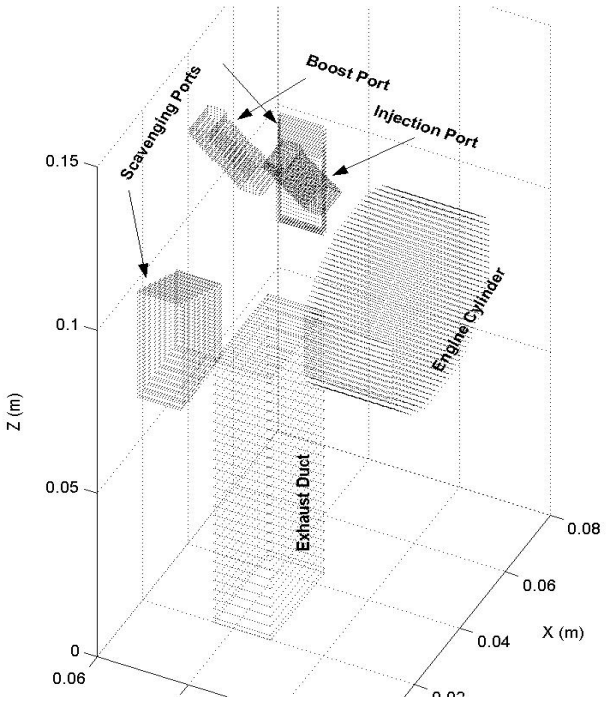


**Figure 3**: *Computational domain at* $100^o$ *ABDC. All the ports and ducts are inactive in the computation at this crankangle.*

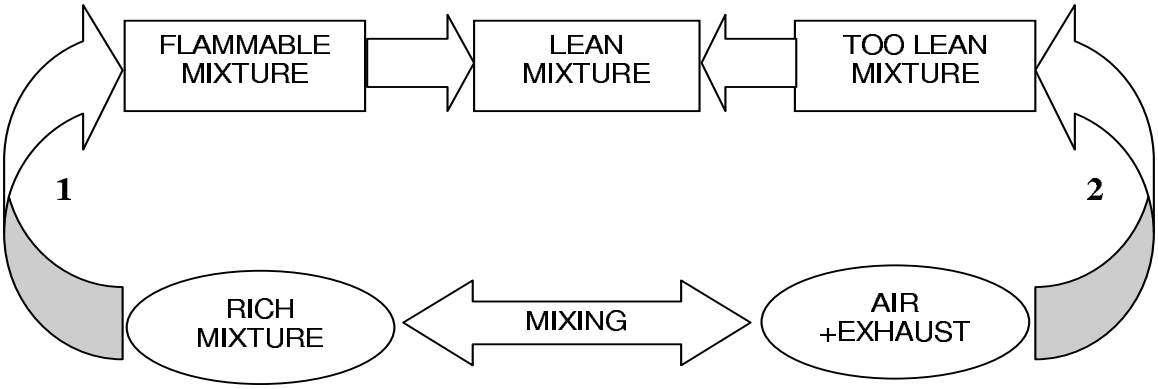


**Figure 4**: *Paths in which the mixing process between rich mixture and air+residual gas progresses.*

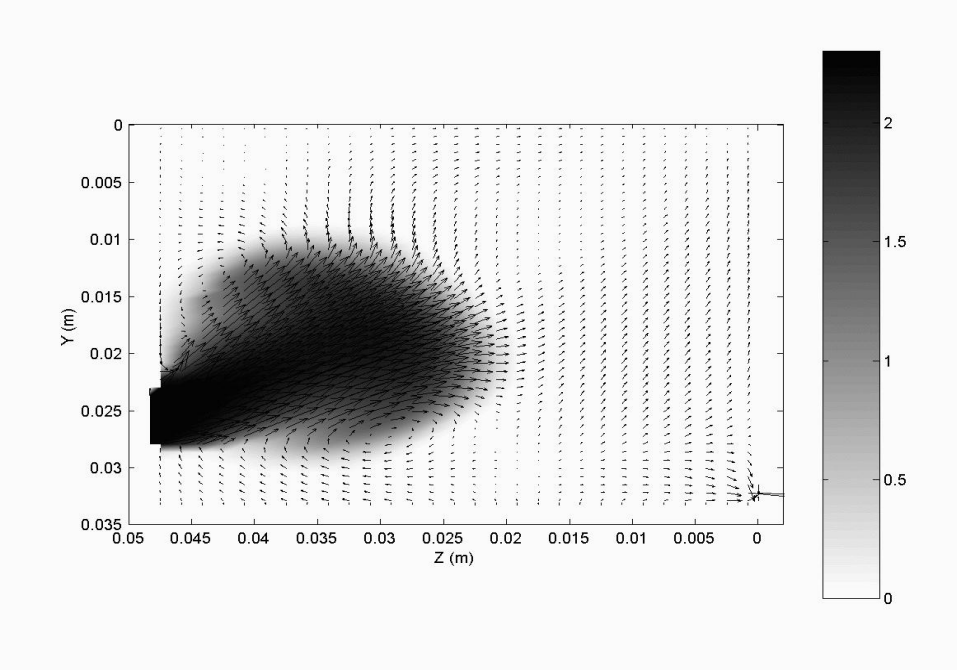


**Figure 5**: *Equivalence ratio colourmap and velocity vectors in Y-Z plane at* $243^o$ *ATDC. The colourbar on the right indicates the value of the equivalence ratio.* $W_{max}$ *= 350 m/s,* $V_{max}$ *= 250 m/s.*

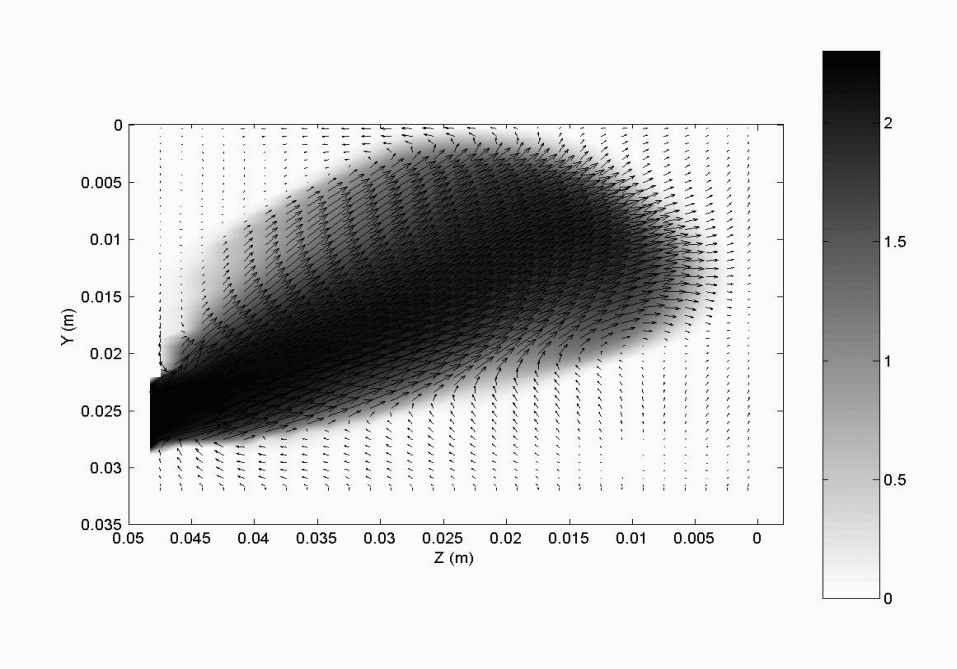


**Figure 6**: *Equivalence ratio colourmap and velocity vectors in Y-Z plane at* $247^o$ *ATDC. The colourbar on the right indicates the value of the equivalence ratio.* $W_{max}$ *= 320 m/s,* $V_{max}$ *= 250 m/s.*

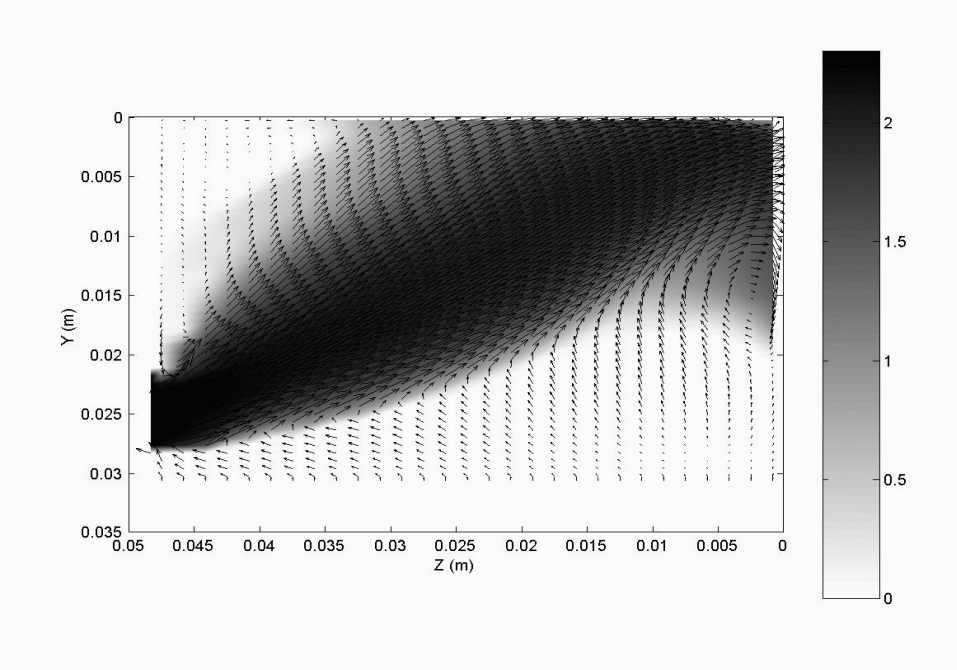


**Figure 7**: *Equivalence ratio colourmap and velocity vectors in Y-Z plane at* $252^o$ *ATDC. The colourbar on the right indicates the value of the equivalence ratio.* $W_{max}$ *= 324 m/s,* $V_{max}$ *= 241 m/s.*

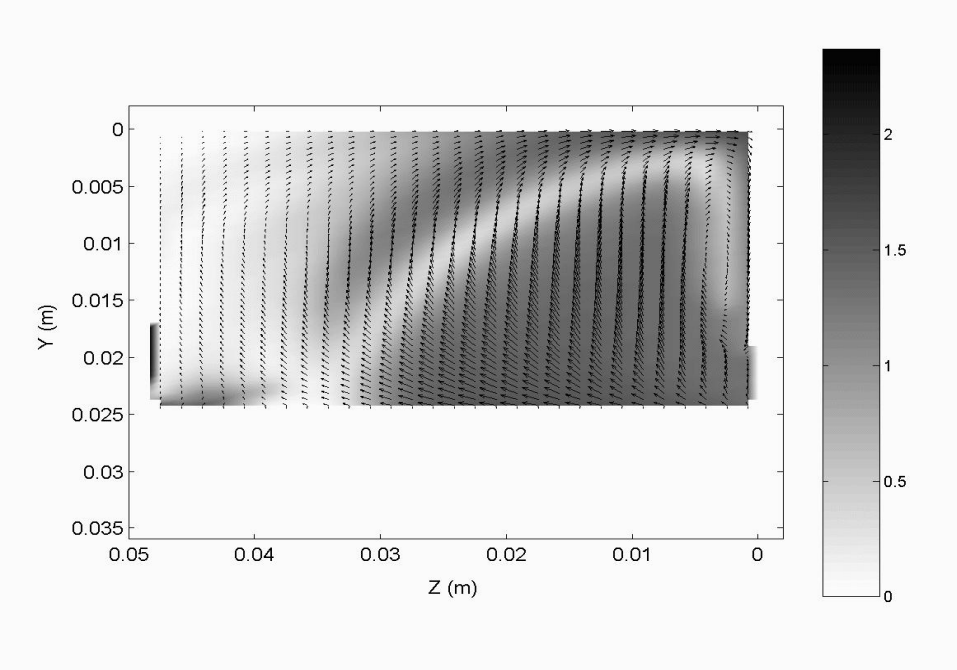


**Figure 8**: *Equivalence ratio colourmap and velocity vectors in Y-Z plane at* $270^o$ *ATDC. The colourbar on the right indicates the value of the equivalence ratio.* $W_{max}$ *= 109 m/s,* $V_{max}$ *= 113 m/s.*

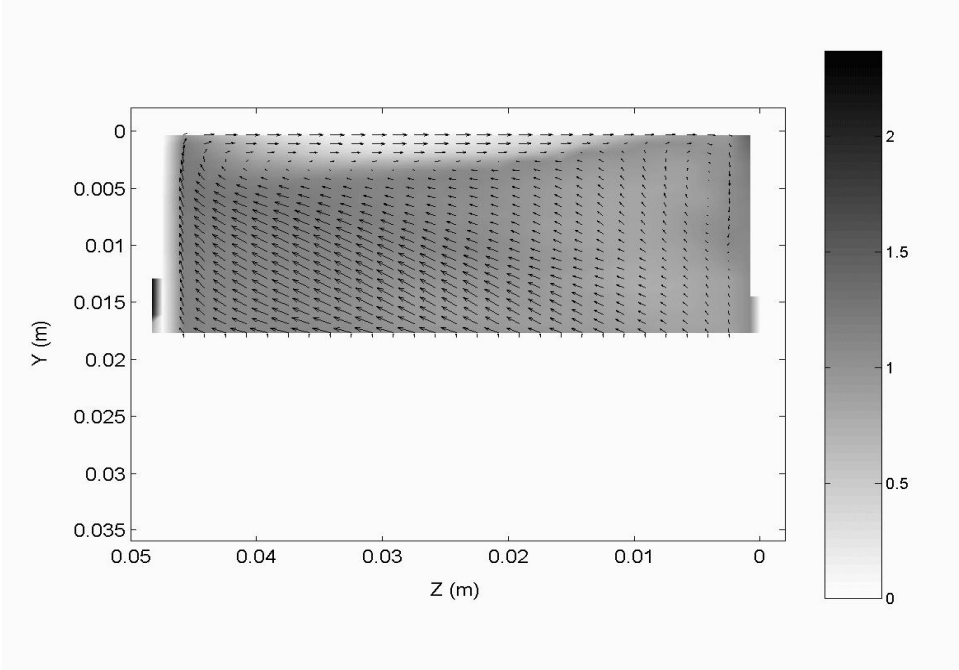


**Figure 9**: *Equivalence ratio colourmap and velocity vectors in Y-Z plane at* $298^o$ *ATDC. The colourbar on the right indicates the value of the equivalence ratio.* $W_{max}$ *= 47 m/s,* $V_{max}$ *= 31 m/s.*

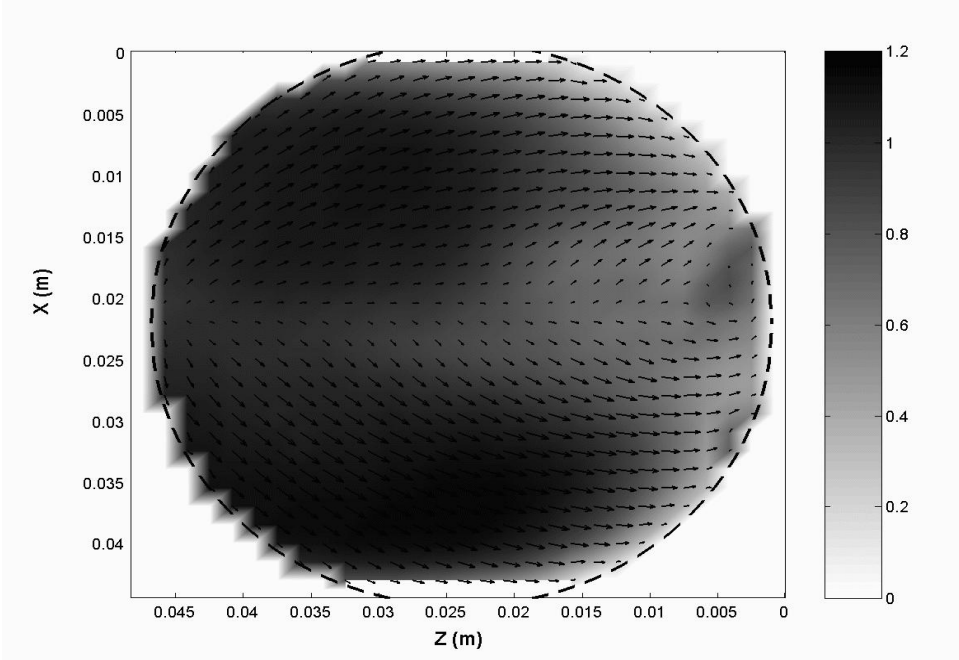


**Figure 10**: *Equivalence ratio colourmap and velocity vectors in X-Z plane at* $340^o$ *ATDC. The colourbar on the right indicates the value of the equivalence ratio.* $W_{max}$ *= 28 m/s,* $V_{max}$ *= 18 m/s.*

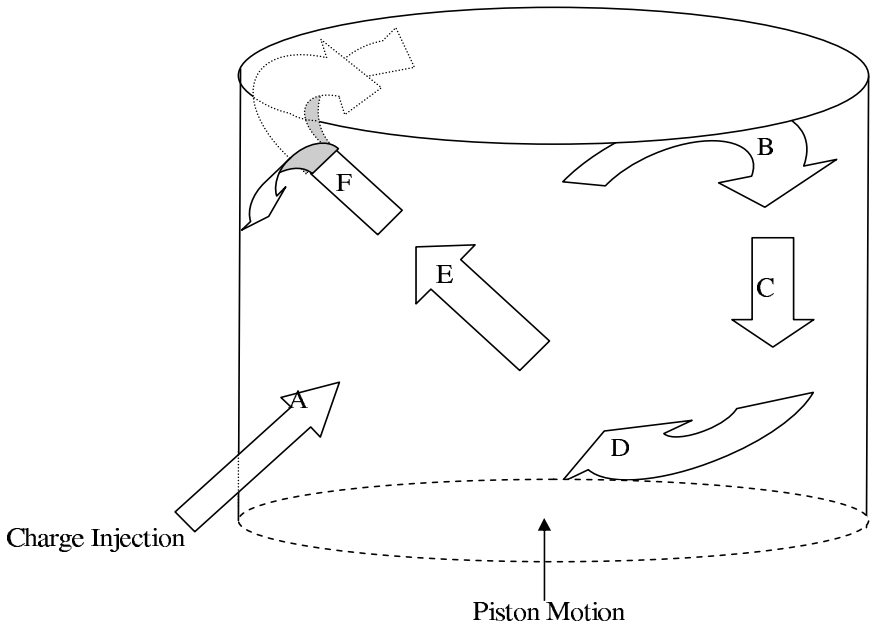


**Figure 11**: *Flow path of the injected charge at high engine speed (6000 rpm).*

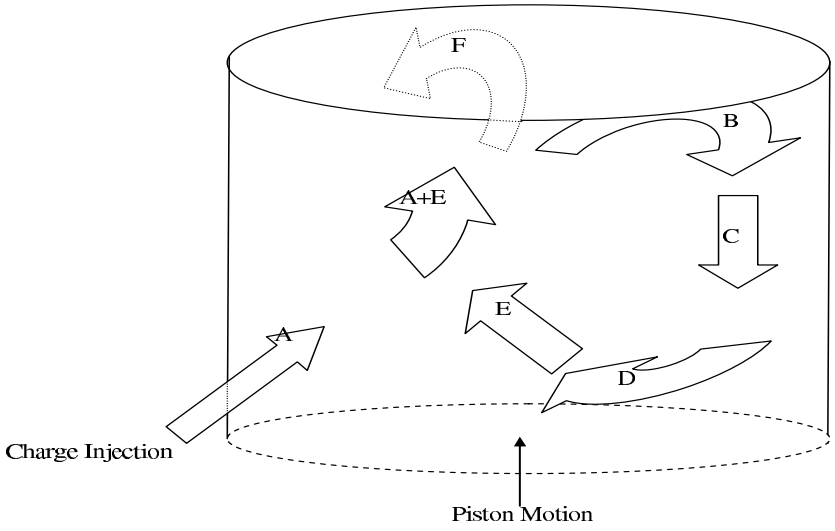


**Figure 12**: *Flow path of the injected charge at low engine speed (2000 rpm).*

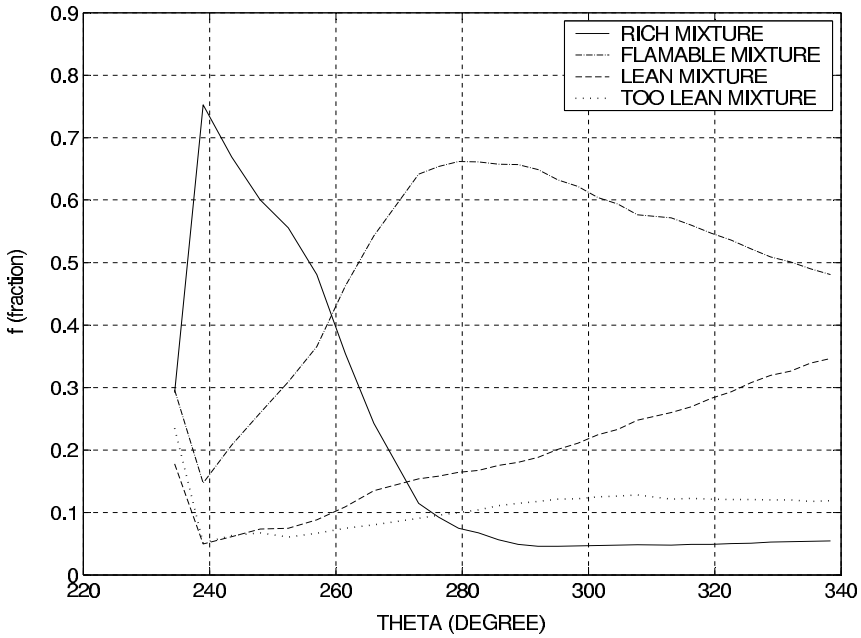


**Figure 13**: *Variation of mass fraction of the relative proportions of fuel-air mixture with crankangle for High Speed High Load (HSHL) condition.*

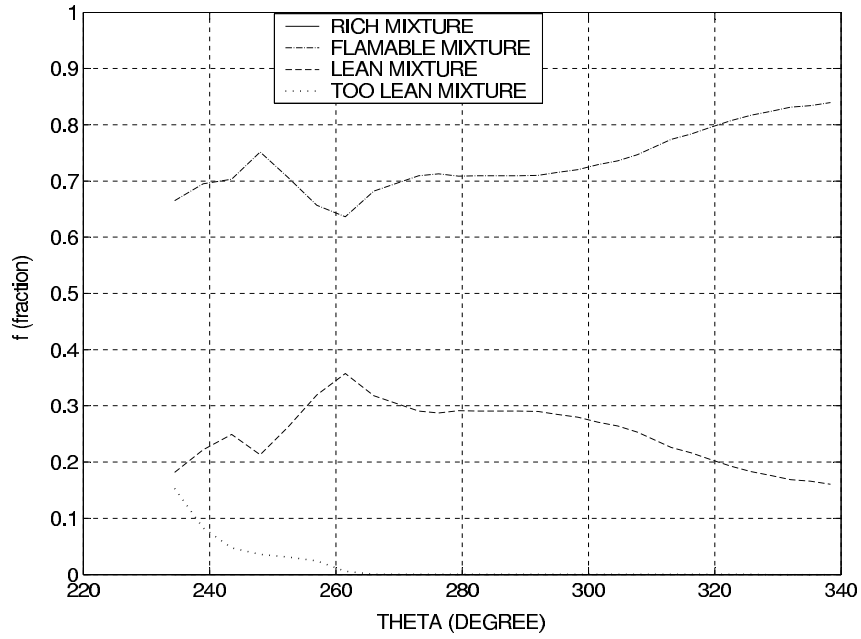


**Figure 14**: *Variation of mass fraction of the relative proportions of fuel-air mixture with crankangle for Low Speed Low Load (LSLL) condition.*

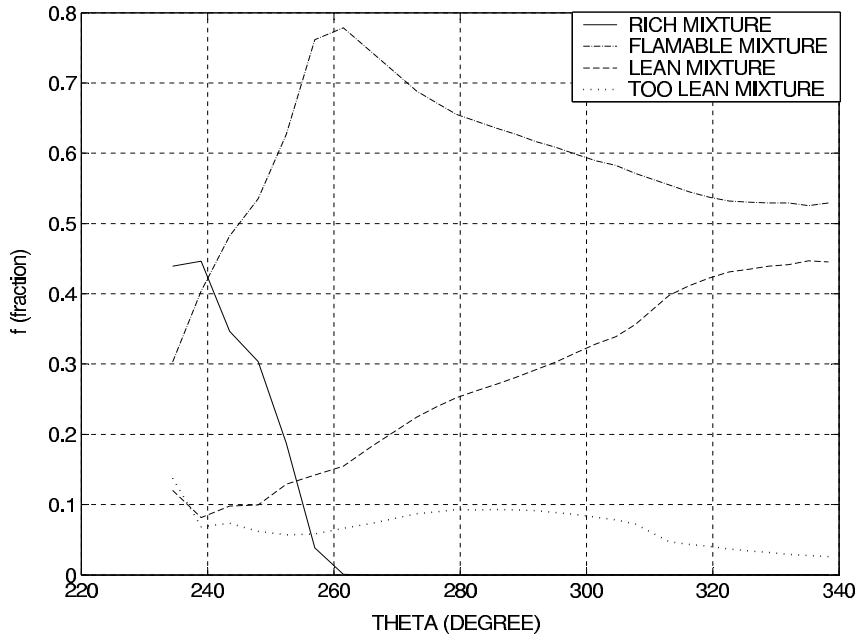


**Figure 15**: *Variation of mass fraction of the relative proportions of fuel-air mixture with crankangle for Mid Speed Mid Load (MSML) condition.*

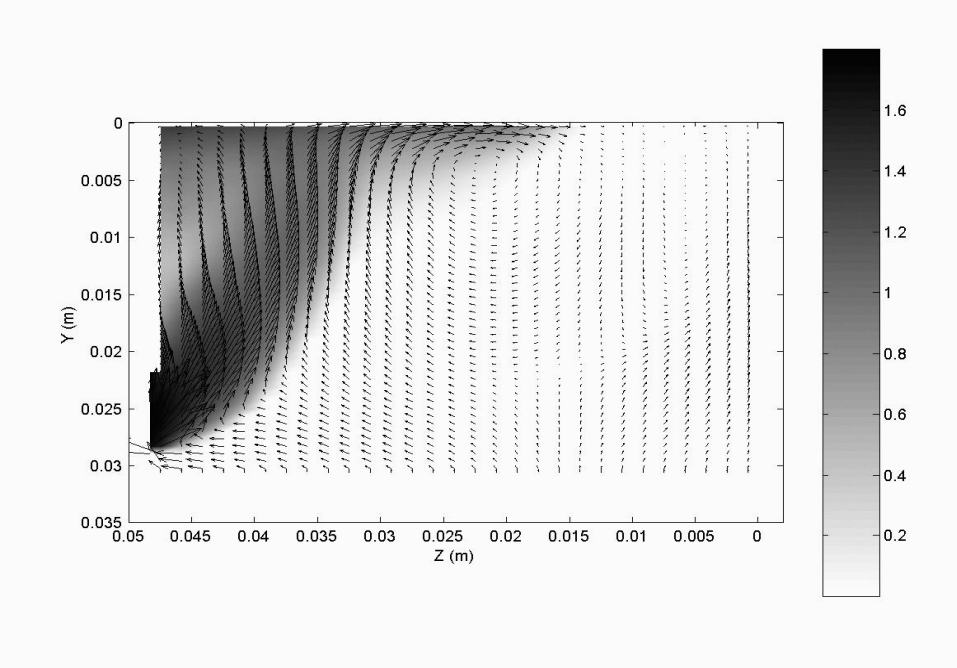


**Figure 16**: *Equivalence ratio colourmap and velocity vectors in Y-Z plane at* $252^o$ *ATDC for an injection angle of* $75^o$ *at Mid Speed Mid Load condition (MSML). The colourbar on the right indicates the value of the equivalence ratio.*

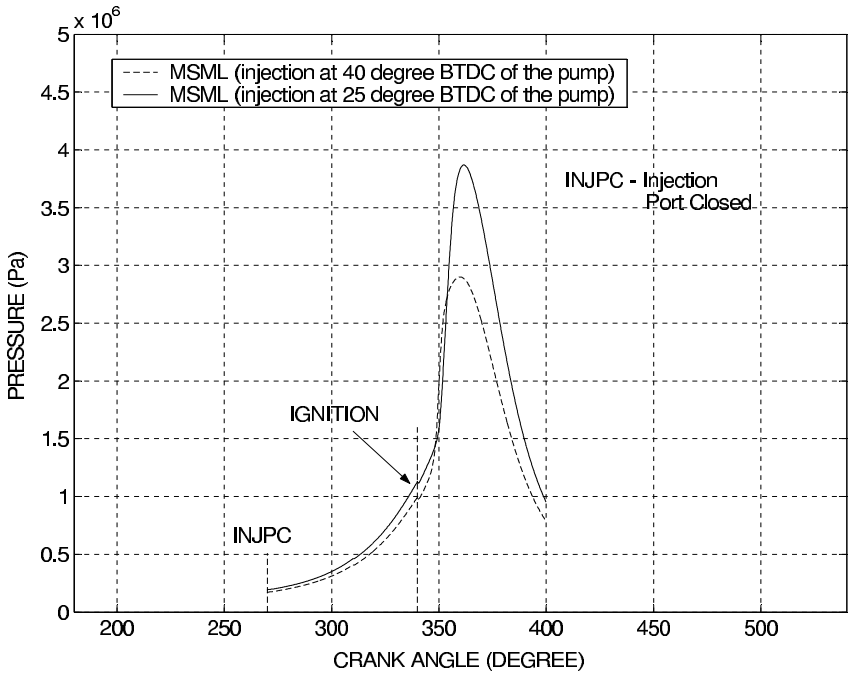


**Figure 17**: *$P - \theta$ prediction for Mid-Speed Mid-Load (MSML) condition. Effect of increased injection pressure.*

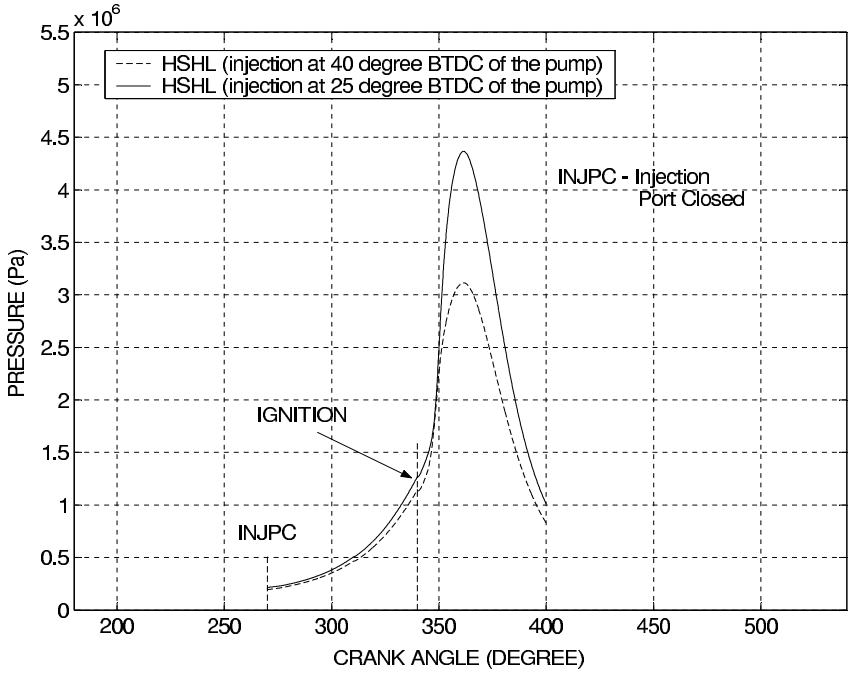


**Figure 18**: *$P - \theta$ prediction for High-Speed High-Load (HSHL) condition. Effect of increased injection pressure.*